Laser flash photolysis of 1,8-bis(substituted methyl)naphthalenes

Akihiko Ouchi,[a] Yoshinori Koga,[a] Maksudul M. Alam[b] and Osamu Ito*[,b]

[a] *National Institute of Materials and Chemical Research, AIST, MITI, Tsukuba, Ibaraki 305, Japan*

[b] *Institute for Chemical Reaction Science, Tohoku University, Katahira, Aoba-ku, Sendai, 980-77, Japan*

The transient absorption spectra obtained by the laser flash photolysis of 1,8-bis(substituted methyl)naphthalenes [(PhX–CH_2)$_2$Naph; X = O, S, Se] have been measured. By comparison with the transient spectra for 1-(substituted methyl)naphthalenes, the transient species absorbing at 430 nm observed from (PhO–CH_2)$_2$Naph is attributed to the triplet state. In the case of (PhS–CH_2)$_2$Naph, absorption bands at 490 and 430 nm due to PhS˙ are observed in addition to an absorption band in the region of 310–400 nm, which is due to the carbon-centred radical [˙CH_2Naph(CH_2–SPh)]. For (PhSe–CH_2)$_2$Naph, a new broad absorption band appeared in the region of 400–520 nm, which covered weak absorption bands due to PhSe˙ at 430 and 490 nm. The new absorption is attributed to the carbon-centred radical [˙CH_2Naph(CH_2–SePh)] in which there is considerable interaction between the ˙CH_2– and PhSe moieties. The possibility of a bridged radical for ˙CH_2Naph(CH_2–SePh) is suggested by MO calculations.

Introduction

Transient spectroscopic methods have often been employed for investigations of intermediates such as excited states and radicals in the photochemical reactions of substituted methylaromatics.[1–7] Most of the methylaromatic compounds intensively studied so far have been mono-substituted derivatives. In non-polar solvents, (halomethyl)naphthalenes have been reported to yield naphthylmethyl radicals.[8,9] The excited states responsible for the cleavage of the carbon–halogen bond have been proposed by various investigators;[10–15] the reaction proceeded from different excited states depending on the wavelength of the photolysis light.

In previous papers, we have reported that acenaphthene is efficiently formed from 1,8-bis(halomethyl)naphthalenes[16–18] and 1,8-(PhX–CH_2)$_2$naphthalenes [abbreviated as (PhX–CH_2)$_2$Naph; X = O, S, Se][19,20] by laser photolysis as shown in Scheme 1. The yield of acenaphthene varied with the

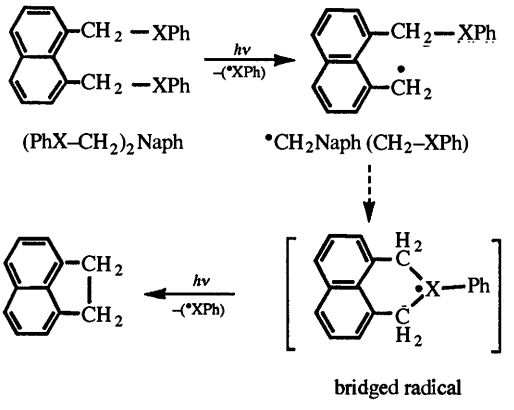

Scheme 1 X = O, S, Se

wavelength and the fluence of the laser light. In general, the order of the efficiency of the photochemical bond-cleavage of PhX–CH_2 was O < S ⩽ Se for (PhX–CH_2)$_2$Naph.[19,20] In order to understand further the reaction mechanism, it is essential to conduct direct observations on the reaction intermediates such as radicals and excited states.

In this study, we report results on the laser flash photolysis of (PhX–CH_2)$_2$Naph. It is interesting to discover whether bridged radicals participate in the reaction, since this might change the character of the intermediate radicals. The transient absorption bands of the intermediates obtained from (PhX–CH_2)$_2$Naph were assigned in comparison with those from 1-(substituted methyl)naphthalenes (PhX–CH_2Naph; X = O, S, Se) and mono-α-substituted toluenes (PhX–CH_2Ph; X = O, S, Se). In addition, semi-empirical MO calculations were performed in order to confirm the interpretation of the experimental results.

Experimental

The solvent used for the transient absorption measurements was spectroscopic grade cyclohexane. 1,8-Bis(PhX–CH_2)naphthalenes were prepared from 1,8-bis(bromomethyl)naphthalene synthesized by the reduction of 1,8-naphthalic anhydride (Wako Chemicals) by $LiAlH_4$ and successive treatment with concentrated HBr. (PhO–CH_2)$_2$Naph was prepared by the reaction of 1,8-bis(bromomethyl)naphthalene with PhOH–K_2CO_3 in acetone. (PhS–CH_2)$_2$Naph was synthesized by the reaction of 1,8-bis(bromomethyl)naphthalene and PhSH–Na in EtOH. (PhSe–CH_2)$_2$Naph was prepared by the reaction of 1,8-bis(bromomethyl)naphthalene and PhSe-SePh–$NaBH_4$ in EtOH. 1-(PhX–CH_2)naphthalenes were prepared similarly from 1-(chloromethyl)naphthalene (Aldrich).

The laser flash photolysis apparatus was a standard design with an Nd:YAG laser of *ca.* 6 ns pulse-duration.[21–23] Solutions were photolysed with FHG light (266 nm) with a laser power of *ca.* 10 mJ. The time profiles were followed using a photomultiplier system. Transient spectra were recorded with a multichannel photo-diode system. Laser photolyses were performed on solutions in a rectangular quartz cell with a 10 mm optical path. The monitoring light was selected using bandpath filters. Solutions were deoxygenated by bubbling through with argon. O_2-Saturated solutions were prepared by bubbling through with oxygen. All the measurements were carried out at 23 °C.

The MO calculations were performed with PM3 and MNDO methods by using MOPAC'93. The electronic transition energies were calculated by INDO method.

Results and discussion

The transient spectra observed after the laser flash photolysis of PhO–CH_2Naph in deaerated cyclohexane with 266 nm light are shown in Fig. 1(*a*). The main transient absorption bands appear at 430 and 400 nm. Both absorption bands were attributed to the same species because their decay rates were similar. In comparison, the transient spectrum observed immediately after the laser flash photolysis of PhO–CH_2Ph is shown in Fig. 1(*b*). The transient absorption band at 390 nm was attributed to PhO$^{\bullet}$ generated as shown in Scheme 2. The slow decay of the

$$PhCH_2\text{–}XPh \xrightarrow{h\nu\,(266\ nm)} Ph\dot{C}H_2 + Ph\dot{X}$$

Scheme 2 X = O, S, Se

390 nm band in aerated solution is consistent with the low reactivity of PhO$^{\bullet}$ with O_2.[24,25]

In contrast, the decay of the 430 and 400 nm bands of PhO–CH_2Naph was accelerated on addition of O_2. The rate constants of the decay in the presence of O_2 and ferrocene (energy of the lowest triplet state E_{T1} = 42.8 kcal mol^{-1})†,[26] were evaluated to be 2.7 × 10^9 and 1.2 × 10^9 dm^3 mol^{-1} s^{-1}, respectively. On addition of isoprene (E_{T1} = 60.1 kcal mol^{-1}), whose triplet energy is slightly higher than that of most naphthalene derivatives (E_{T1} = 58–59 kcal mol^{-1}),[27] the decay was not accelerated. These findings indicate that the bands at 430 and 400 nm can be attributed to the triplet state of PhO–CH_2Naph. In Scheme 3, two possible paths are shown for the

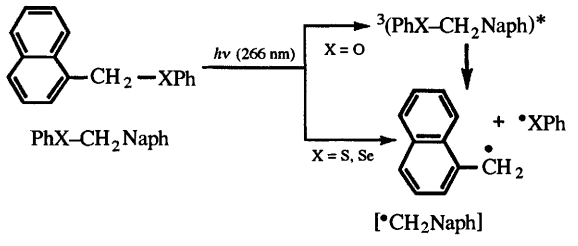

Scheme 3

excitation of PhX–CH_2Naph; the triplet route is the main one in the case of X = O.

These results indicate that the C–O bond of PhO–CH_2Ph is more photo-dissociative than that of PhO–CH_2Naph. This can be explained by a difference between the energy levels between the T_1 state and the dissociation curve for the two compounds; for PhO–CH_2Ph, the excited energy flows down to the dissociative curve which is lower in energy than the T_1 state, leading to easy dissociation. However, the T_1 state of PhO–CH_2Naph is lower in energy than the dissociative curve, resulting in an accumulation of the T_1 state.

In the laser flash photolysis of (PhO–CH_2)$_2$Naph, the transient absorption bands shown in Fig. 2 were observed. The absorption band at 430 nm with a shoulder at 400 nm is similar to the triplet–triplet band of PhO–CH_2Naph. The decay was also accelerated by the addition of triplet quenchers with lower E_{T1} than that of most naphthalene derivatives. An example is shown in the decay curves (insert in Fig. 2) in the absence and presence of air. Thus, the main transient absorption band is attributed to the triplet state.

In the region of 310–380 nm, transient absorption bands with slow decay were observed. The intensity of the band decreased with the addition of oxygen, suggesting that they were produced *via* an O_2-reactive precursor such as the triplet state. A plausible species for the absorption is a naphthylmethyl-type radical. However, the observed slow decay in aerated solution indicates

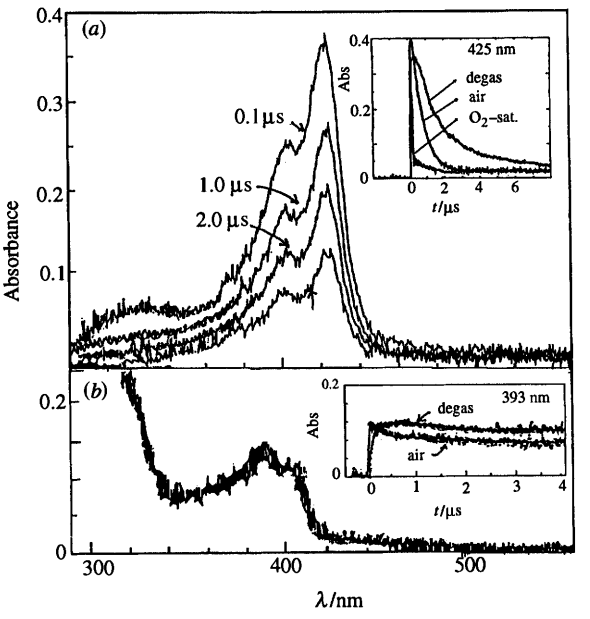

Fig. 1 Transient absorption spectra observed by laser photolysis with 266 nm light in deaerated cyclohexane. (*a*) PhO–CH_2Naph (1 mmol dm^{-3}) and (*b*) PhO–CH_2Ph (1 mmol dm^{-3}). Insert: decay profiles.

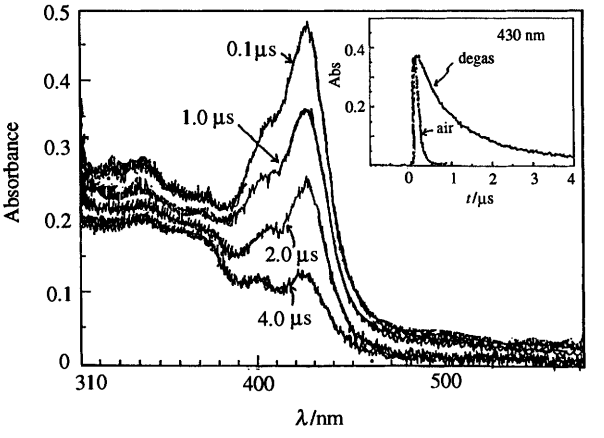

Fig. 2 Transient absorption spectra observed by laser photolysis of (PhO–CH_2)$_2$Naph (1 mmol dm^{-3}) with 266 nm light in deaerated cyclohexane. Insert: decay profiles.

that the absorption bands are not due to the triplet state or to the usual carbon-centred radicals. The absorption of PhO$^{\bullet}$ may overlap with these absorptions, which makes further analysis difficult.

Fig. 3 shows the transient absorption bands observed after the laser flash photolysis of PhS–CH_2Ph and PhS–CH_2Naph. The broad bands of PhS–CH_2Ph in the region of 400–520 nm with peaks at 450 and 490 nm were assigned to PhS$^{\bullet}$ (Scheme 2) because these bands were insensitive to O_2, which is a typical property of PhS$^{\bullet}$.[28–30]

The transient absorption bands of PhS–CH_2Naph in the region of 400–520 nm were also ascribed to PhS$^{\bullet}$ because they were not much affected by air, which also indicates the absence of the triplet state. This indicates that bond dissociation occurs between the C–S bond of PhS–CH_2Naph, which is shown as the radical route in Scheme 3. The absorption band at 350 nm was attributed to the carbon-centred radical [$^{\bullet}$$CH_2$Naph],[10–12] because the absorption intensity decreased on addition of O_2.[31] The decrease in the absorption intensity suggests the existence of a very fast reaction with O_2, although the decay was not accelerated by O_2 as seen in the inserted time profiles. The slow decay part may be due to the absorption of PhS$^{\bullet}$.

Compared with PhO–CH_2Naph, which predominantly formed the triplet state, the S–C bond in PhS–CH_2Naph

† 1 cal = 4.184 J.

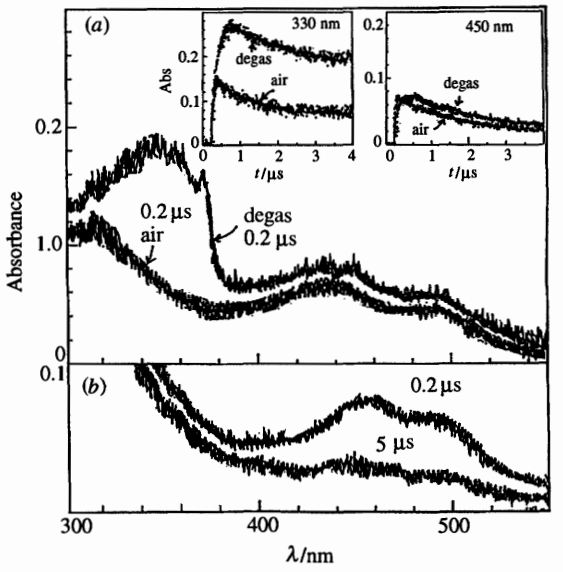

Fig. 3 Transient absorption spectra observed by laser photolysis with 266 nm light. (*a*) PhS–CH_2Naph (1 mmol dm^{-3}) in aerated and deaerated cyclohexane. (*b*) PhS–CH_2Ph (1 mmol dm^{-3}) in deaerated cyclohexane. Insert: decay profiles.

dissociated easily because of the presence of a C–S bond which is weak compared with the relatively strong C–O bond. The weakness of the C–S bond can be inferred from the lower resonance energy of PhS$^{\bullet}$ compared with that of PhO$^{\bullet}$.[32,33] In the case of PhS–CH_2Naph, the dissociative curve may be lower in energy than the T_1 state.

Fig. 4 shows the transient absorption spectra of (PhS–CH_2)$_2$Naph. The absorption bands in the region of 400–520 nm were attributed to PhS$^{\bullet}$. The absorption band in the region of 320–400 nm observed in aerated solution was due either to PhS$^{\bullet}$ or to acenaphthene. In deoxygenated solution, the absorption bands in the region of 310–400 nm with peaks at 340 and 370 nm were attributed to the carbon-centred radical, $^{\bullet}CH_2$Naph(CH_2–SPh);[10–12] this was confirmed by the increase in the decay rate on addition of O_2. In the case of $^{\bullet}CH_2$Naph(CH_2–SPh), the 2p orbital of $^{\bullet}CH_2$ may not always be fixed in the same plane as the naphthalene π-orbitals for steric reasons. Thus, the absorption bands of $^{\bullet}CH_2$Naph(CH_2–SPh) are not necessarily going to be similar to those of $^{\bullet}CH_2$Naph. However, the absorption bands of these carbon-centred radicals appeared in the same region. The potential curve of (PhS–CH_2)$_2$Naph, which dissociates into PhS$^{\bullet}$ and $^{\bullet}CH_2$Naph(CH_2–SPh), should be lower in energy than that of the T_1 state.

The transient absorption spectra of PhSe–CH_2Ph and PhSe–CH_2Naph are shown in Fig. 5. The formation of PhSe$^{\bullet}$ was confirmed by the absorption band in the region of 400–520 nm, which was insensitive to O_2.[34] The insensitivity of the band to O_2 indicates the absence of the triplet state. The absorption band observed on the laser flash photolysis of PhSe–CH_2Naph in the shorter wavelength region (330–380 nm) was attributed to $^{\bullet}CH_2$Naph; this is the result of the C–Se bond cleavage, which took place on laser photolysis.

The transient absorption spectra observed from (PhSe–CH_2)$_2$Naph are shown in Fig. 6(*a*), in which the absorption spectrum of PhSe$^{\bullet}$ is also depicted. The transient absorption band of (PhSe–CH_2)$_2$Naph in the region of 400–520 nm becomes broad and intense in both aerated and deaerated solutions compared with that of PhSe$^{\bullet}$; the shape of the transient absorption of (PhSe–CH_2)$_2$Naph is different from that of the triplet state for a naphthalene moiety. For (PhSe–CH_2)$_2$Naph, a broad absorption with a maximum at 450 nm was obtained after subtracting the absorption of PhSe$^{\bullet}$ from the absorption in aerated solution [Fig. 6(*b*)]. The absorption

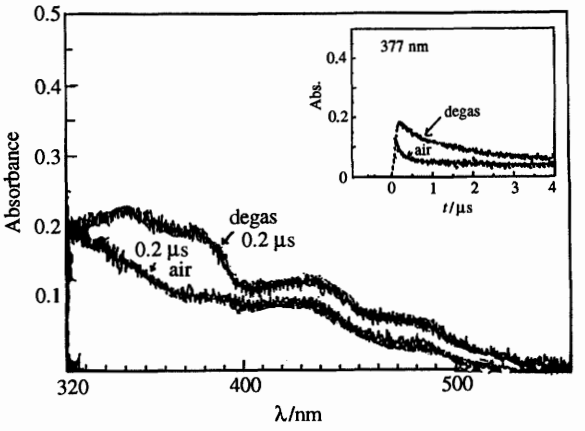

Fig. 4 Transient absorption spectra observed by laser photolysis of (PhS–CH_2)$_2$Naph (1 mmol dm^{-3}) with 266 nm light in aerated and deaerated cyclohexane. Insert: decay profiles.

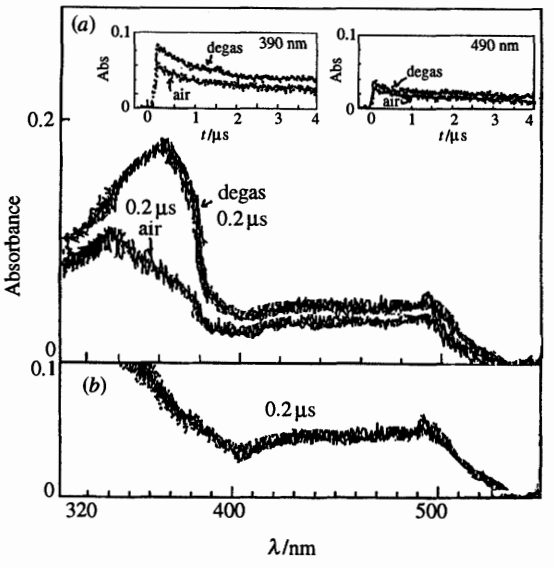

Fig. 5 Transient absorption spectra observed by laser photolysis with 266 nm light in aerated and deaerated cyclohexane. (*a*) PhSe–CH_2Naph (1 mmol dm^{-3}) and (*b*) PhSe–CH_2Ph (1 mmol dm^{-3}). Insert: decay profiles.

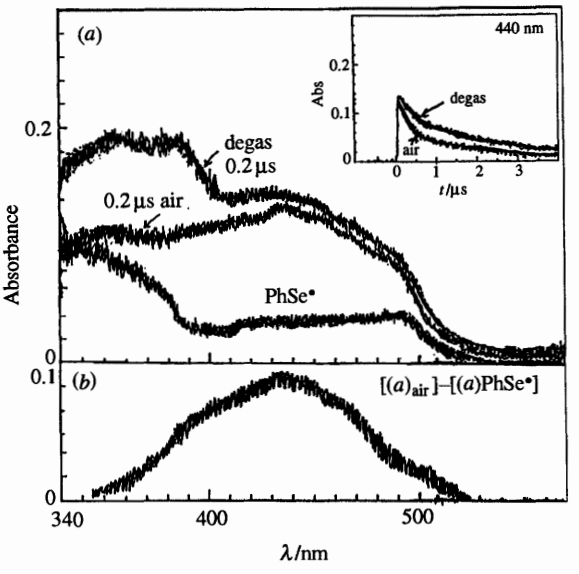

Fig. 6 (*a*) Transient absorption spectra observed by the laser photolysis of (PhSe–CH_2)$_2$Naph (1 mmol dm^{-3}) with 266 nm light in aerated and deaerated cyclohexane. Insert: decay profiles. The spectrum of PhSe$^{\bullet}$ shown is that from Fig. 5 in aerated solution. (*b*) The difference spectrum was obtained by subtracting the spectrum of PhSe$^{\bullet}$ from that in aerated solution.

bands in the shorter wavelength region [320–400 nm in Fig. 6(*a*)] show typical carbon-centred radical behaviour.

In the decay time profile in Fig. 6(*a*), the decay rate at 400–520 nm was increased by the initial addition of O_2. This result suggests that the species responsible for the band at 400–520 nm has partial carbon-centred radical character. Assuming a bridged radical is responsible for the absorption bands at 400–520 nm, the unpaired electron may disperse among the α-carbon atoms and the selenium atom. Thus, such a bridged radical may have intermediate character between a carbon radical and PhSe$^{\bullet}$. Indeed, the decay seen in the time profile [insert to Fig. 6(*a*)] was clearly faster than that of pure PhSe$^{\bullet}$, but the decay was slower than that of a pure carbon radical in the presence of O_2 (Fig. 5). Therefore, the broad band shown in Fig. 6(*b*) suggests the formation of a bridged radical.

If 1,8-naphthoquinodimethane was formed by a two photon process, the main absorption bands would be expected to appear in the region of 350–300 nm in addition to a weak band around 500 nm.[35] In this case, the bands in both these regions should behave in the same way when O_2 is present; however, the observed decays were different (Fig. 6). Thus, the formation of 1,8-naphthoquinodimethane is improbable.

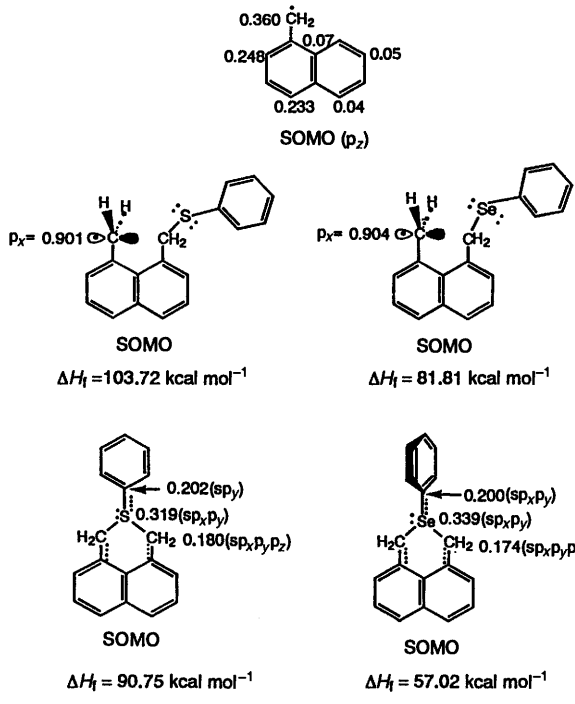

Fig. 7 Heat of formation (ΔH_f) and unpaired electron density of the SOMO for the non-bridged and bridged radicals of $^{\bullet}CH_2Naph(CH_2–XPh)$; the π-orbitals of naphthalene ring are fixed to p_z

In order to reveal the structures of the radical species, MO calculations were performed by PM3 and MNDO methods. The heat of formation (ΔH_f) of the radicals and the distribution of the unpaired electron of the singly occupied molecular orbital (SOMO) are summarized in Fig. 7. For $^{\bullet}CH_2Naph(CH_2–XPh)$, when the geometry optimization was started from non-bridged radicals, the open radical structures shown in Fig. 7 were obtained. The unpaired electron of the SOMO of non-bridged radicals mainly localizes on the 1-methyl p_x-orbital which is perpendicular to the naphthalene p_z-orbitals. On the other hand, the bridged structures were obtained when optimization was started from the closed form for three of the $^{\bullet}CH_2Naph(CH_2–XPh)$ radicals. In the case of the bridged $^{\bullet}CH_2Naph(CH_2–SPh)$, the most stable conformation of the radical was a planar structure in which the phenyl is in the same plane as the naphthalene. The ΔH_f value of the twisted phenyl conformer of the bridged $^{\bullet}CH_2Naph(CH_2–SePh)$ was slightly lower than that of the planar structure. For X = O, the ΔH_f value of the bridged radical is greater than the non-bridged one, while the ΔH_f values of bridged form for X = S and Se are lower than those of the corresponding non-bridged ones. The difference in the ΔH_f values between the bridged and non-bridged radicals for $^{\bullet}CH_2Naph(CH_2–SePh)$ is larger than that of $^{\bullet}CH_2Naph(CH_2–SPh)$, suggesting that the bridged form of the former is more favourable than that of the latter. In the SOMO of the bridged radicals, the unpaired electron delocalizes mainly on the S or Se atoms and the three adjacent carbon atoms.

The electronic transition energies of the radicals were calculated by the INDO method; however, the calculated ν_{max} did not reproduce the observed value even for the naphthylmethyl radical. For the open radical of $^{\bullet}CH_2Naph(CH_2–XPh)$, the λ_{max} is expected at a shorter wavelength, because of the localized p_x-orbital at the 1-methyl radical centre. In the case of the bridged radical, it would be expected that the λ_{max} would appear at a longer wavelength region because the unpaired electron delocalizes on the X atom and its three neighbouring carbon atoms.

The observed photochemistry is explained by the potential energy diagrams schematically shown in Fig. 8. For PhX–CH_2Ph (X = O, S, Se), the dissociative potential curve is at a lower energy than the excited states such as S_1 and T_1. Because the absorption bands of PhX$^{\bullet}$ appeared immediately after the laser pulse, the precursor of the radicals may be the S_1-state rather than the T_1-state. For PhO–CH_2Naph and (PhO–CH_2)$_2$Naph, the T_1 levels are slightly lower than the dissociative curves, predominantly generating the lowest triplet state. When X = S and Se for PhX–CH_2Naph and (PhX–CH_2)$_2$Naph, the dissociative curves are lower than the excited states such as the S_1- and T_1-energy levels.

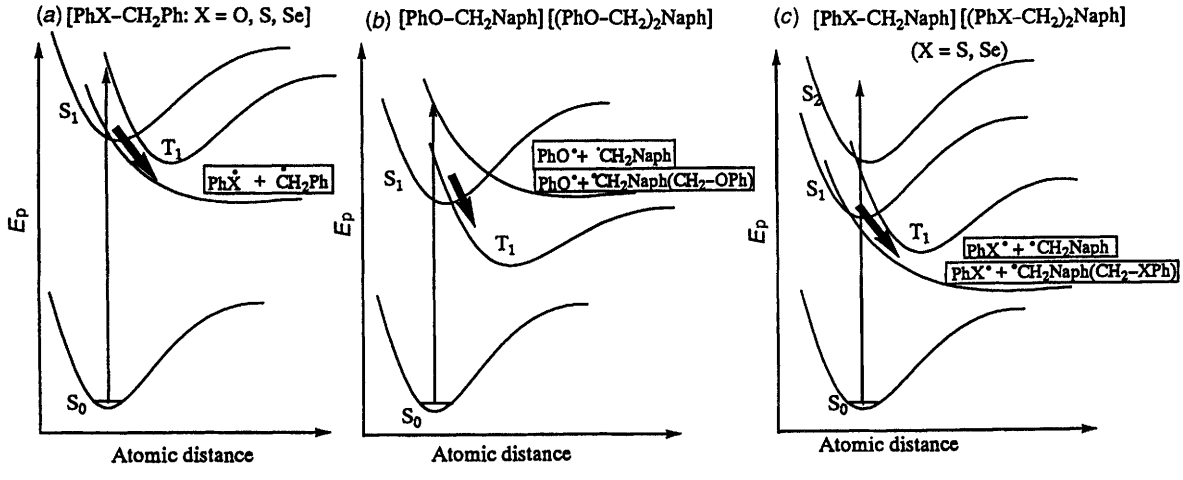

Fig. 8 Schematic illustration of potential energy diagrams for PhX–CH_2Ph, PhX–CH_2Naph and (PhX–CH_2)$_2$Naph

Conclusions

For all the PhX–CH_2Ph compounds studied, photo-dissociation was the predominant process. Facile photo-dissociation occurred at the carbon–X bonds of PhX–CH_2Naph and (PhX–CH_2)$_2$Naph for X = S and Se, whereas the main process for X = O was triplet state formation. For (PhS–CH_2)$_2$Naph, the non-bridged form of $^{\bullet}CH_2$Naph(CH_2–SPh) was the major component in the photolysis, while the bridged form of $^{\bullet}CH_2$Naph(CH_2–SePh) was the major component in the photolysis of (PhSe–CH_2)$_2$Naph.

Acknowledgements

The authors acknowledge the use of MOPAC'93 the source of which was Dr J. J. P. Stewart and Fujitsu Limited, Tokyo, Japan.

References

1 A. Bromberg, K. H. Schmidt and D. Meisel, *J. Am. Chem. Soc.*, 1985, **107**, 83.
2 K. Tokumura, N. Mizukami, M. Udagawa and M. Itoh, *J. Phys. Chem.*, 1986, **90**, 3873.
3 D. Meisel, P. K. Das, G. L. Hug, K. Bhattacharyya and R. W. Fessenden, *J. Am. Chem. Soc.*, 1986, **108**, 4706.
4 K. Tokumura, M. Udagawa, T. Ozaki and M. Itoh, *Chem. Phys. Lett.*, 1987, **141**, 558.
5 D. Weir, L. J. Johnston and J. C. Scaiano, *J. Phys. Chem.*, 1988, **92**, 1742.
6 K. Tokumura and M. Itoh, *Nippon Kagaku Kaishi*, 1989, 1311.
7 K. Tokumura, T. Ozaki, M. Udagawa and M. Itoh, *J. Phys. Chem.*, 1989, **93**, 161.
8 J. C. Scaiano and L. J. Johnston, *Pure Appl. Chem.*, 1986, **58**, 1273.
9 L. van Haelst, E. Haselbach and P. Suppan, *Chimia*, 1988, **42**, 231.
10 G. H. Slocum and G. B. Schuster, *J. Org. Chem.*, 1984, **49**, 2177.
11 L. J. Johnston and J. C. Scaiano, *J. Am. Chem. Soc.*, 1985, **107**, 6368.
12 K. Tokumura, M. Udagawa and M. Itoh, *J. Phys. Chem.*, 1985, **89**, 5147.
13 A. Kawai, T. Okutsu and K. Obi, *Chem. Phys. Lett.*, 1990, **174**, 213.
14 D. F. Kelley, S. V. Milton, D. Huppert and P. M. Rentzepis, *J. Phys. Chem.*, 1983, **87**, 1842.
15 E. F. Hilinski, D. Huppert, D. F. Kelley, S. V. Milton and P. M. Rentzepis, *J. Am. Chem. Soc.*, 1984, **106**, 1951.
16 A. Ouchi and A. Yabe, *Tetrahedron Lett.*, 1990, **31**, 1727; 1992, **33**, 5359; *Chem. Lett.*, 1995, 945.
17 W. Adam and A. Ouchi, *Tetrahedron Lett.*, 1992, **33**, 1875.
18 O. Ito, M. M. Alam, Y. Koga and A. Ouchi, *J. Photochem. Photobiol. A.*, in the press.
19 A. Ouchi and W. Adam, *J. Chem. Soc., Chem. Commun.*, 1993, 628.
20 A. Ouchi, A. Yabe and W. Adam, *Tetrahedron Lett.*, 1994, **34**, 6309; A. Ouchi and Y. Koga, *Tetrahedron Lett.*, 1995, **36**, 8999.
21 A. Watanabe and O. Ito, *J. Phys. Chem.*, 1994, **98**, 7736.
22 M. M. Alam, A. Watanabe and O. Ito, *J. Org. Chem.*, 1995, **60**, 3440.
23 O. Ito, Y. Sasaki, Y. Yoshikawa and A. Watanabe, *J. Phys. Chem.*, 1995, **99**, 9838.
24 E. J. Land, G. Porter and E. Strachan, *Trans. Faraday Soc.*, 1961, **57**, 1885.
25 E. J. Land and G. Porter, *Trans. Faraday Soc.*, 1963, **59**, 2016.
26 A. Familo and F. Wilkinson, *Chem. Phys. Lett.*, 1975, **34**, 575.
27 S. I. Murov, *Handbook of Photochemistry*, Marcel Dekker, New York, 1973.
28 F. C. Thyrion, *J. Phys. Chem.*, 1973, **77**, 1478.
29 O. Ito and M. Matsuda, *J. Am. Chem. Soc.*, 1979, **101**, 1815.
30 C. Chatgilialoglu and K. D. Asmus, *Sulfur-Centered Reactive Intermediates in Chemistry and Biology*, NATO ASI Series A, *Life and Science*, Plenum Press, New York, 1990; vol. 197, pp. 327–340.
31 B. Millard, K. U. Ingold and J. C. Scaiano, *J. Am. Chem. Soc.*, 1983, **105**, 5095.
32 S. W. Benson, *Methods for the Estimation of Thermodynamic Data and Rate Parameters*, Wiley, New York, 1971.
33 A. J. Colussi and S. W. Benson, *Int. J. Chem. Kinet.*, 1977, **9**, 295.
34 O. Ito, *J. Am. Chem. Soc.*, 1983, **105**, 850.
35 M. C. Biewer, M. S. Platz, M. Roth and J. Wirz, *J. Am. Chem. Soc.*, 1991, **113**, 8069.

Paper 5/08251J
Received 19*th December* 1995
Accepted 1*st April* 1996